Asian Journal of Chemistry; Vol. 27, No. 11 (2015), 4153-4159

ASIAN JOURNAL OF CHEMISTRY

http://dx.doi.org/10.14233/ajchem.2015.19172

A Facile Fast Fourier Transforms Method for Characterization of Nanoporous Templates

JINGLEI LEI[1], SHENGMAO WU[1], LINGJIE LI[1,*], GUANYU LI[1] and NIANBING LI[2]

[1]School of Chemistry and Chemical Engineering, Chongqing University, Chongqing 400044, P.R. China
[2]School of Chemistry and Chemical Engineering, Southwest University, Chongqing 400715, P.R. China

*Corresponding author: Fax: +86 23 65112328; Tel: +86 15023661557; E-mail: ljli@cqu.edu.cn

Received: 13 March 2015; *Accepted*: 6 May 2015; *Published online*: 16 July 2015; AJC-17423

High-quality nanoporous templates play an important role in nanomaterials. However, it is difficult to quantitatively evaluate the quality of nanotemplates. In this work, a method based on image processing technology and frequency-domain analysis method is proposed. The geometric parameters of templates including porosity, diameters are extracted. To evaluate the pores ordering, two parameters, the characteristic angle and peak-peak ratio are proposed by combining two-dimensional fast Fourier transforms (2-D FFT) and 1-D fast Fourier transforms techniques. According to the parameters, the lattice type and the pores ordering can be inferred. The accuracy and reliability of present method have been verified by analyzing a standard test image. After that, the quality of some anodic aluminum oxide templates is effectively assessed. The results show this method provides a facile, reliable and comprehensive approach to evaluate the quality of nanoporous templates, which is helpful to optimize the preparation technology and to prepare high-performance functional nanomaterials.

Keywords: Nanoporous templates, Image processing, Frequency-domain analysis, Fast Fourier transforms, Anodic aluminum oxide.

INTRODUCTION

Nanoporous templates, *e.g.*, anodic aluminum oxide (AAO) templates are widely used to fabricate one- or two-dimensional nanostructured materials such as nanorods, nanowires, nanotubes and nanomesh[1-5]. Due to its simplicity and low cost[6], the template-synthesis method has been an effective approach to prepare high-performance functional nanomaterials for catalysis, high density magnetic recording, photonic materials, sensors, *etc*.[7-12]. Generally, the quality of the nanoporous templates depends on the preparation conditions and has great effects on the performance of functional nanomaterials[13]. Therefore, in order to optimize the template preparation conditions and improve the performance of the functional nanomaterials, the quality of a nanoporous template is expected to evaluate quantitatively.

On usual, evaluating the quality of a nanoporous template mainly contains two aspects. One is to extract geometric size parameters such as the porosity, the diameters and their variance of pores. There are many reports on this aspect and these parameters are easily obtained by analyzing the top-view microscopic images of scanning electron microscope (SEM) or atomic force microscope (AFM) of the template with some softwares (even free softwares such as ImageJ)[14]. The other is to characterize the degree of ordering of the pores in the nanoporous template, which is much difficult and attracts much attention recently.

To characterize the ordering of pores in a nanoporous template, generally, there are two approaches. The first one is to calculate some particular ordering parameters from the morphology image. Hillebrand *et al.*[15] proposed a method based on the distances between nearest neighbours and angular order of pores. They proposed the parameters *Dev_d* and *Dev_*α to analyze the grain morphology in hexagonal lattices. This method was also used by other researchers to analyze the orientational distribution of pores successfully[16]. On the basis of Hillebrand method, Abdollahifard *et al.*[17] developed a histogram-based segmentation method for evaluating the degree of ordering of the hexagonal nanoporous anodic aluminum oxide lattices, which significantly improves the robustness of the method. However, both above methods are complex and sensitive to the ordering tolerance parameter, which is an arbitrary threshold parameter. To avoid the threshold parameter, Pourfard *et al.*[18] used a statistical method and Borba *et al.*[19] proposed a local ordering parameter based on statistical mechanics, respectively. It should be pointed out that all the methods mentioned above are only suitable for the hexagonal lattice and are difficult to analyze other lattices.

The other approach for characterizing the ordering degree of the pores is based on the two-dimensional fast Fourier

transforms (2-D FFT), which transforms the morphology images from the spatial domain to the frequency domain. Sulka *et al.*[20] analyzed the field-emission scanning electron microscope (FE-SEM) images of porous alumina membranes and evaluated the regularity of the pores arrangement through the evolution of the fast Fourier transforms patterns. Rahimi *et al.*[21] employed the linear-angular fast Fourier transforms to acquire the ordering degree of the porous anodized alumina prepared under various conditions. These methods allow a qualitative characterization of the lattice type in a small region. However, as for the situation in a large region, the treatment results are unsatisfied because the 2-D fast Fourier transforms patterns tend to be the similar shapes[18].

Here we present a new and comprehensive fast Fourier transforms method to analyze quantitatively the quality of pores in nanoporous templates. The geometric parameters of pores are extracted reliably by statistically analyzing every pixel of the microscopic image of templates. To characterize the ordering degree of the pores, a facile algorithm combing 1-D fast Fourier transforms and 2-D fast Fourier transforms is proposed for the first time. Due to employing 1-D fast Fourier transforms technique after 2-D fast Fourier transforms analysis, the method can deal with the problems that the similar shapes in the 2-D patterns, which makes it suitable for evaluation of the orientational ordering of pores not just in the short-range region but in the long-range region and for quantitatively describing the ordering degree of pores not only for the hexagonal lattice but for other lattices such as square lattice. Moreover, we achieved our algorithm automatically and reliably with MATLAB software. After the morphologic image of a template is inputted, all the geometric and oriental parameters can be calculated for evaluating the quality of the template.

EXPERIMENTAL

The general method to analyze the morphology image of a nanoporous template is described here. The algorithm includes two parts: (i) extracting the geometric parameters by the image processing which include the porosity, diameters and their variance of pores; (ii) obtaining the ordering parameters based on fast Fourier transforms technique.

Image preprocessing: A typical SEM or AFM image is an image with the gray-scale value from 0 to 255. If we extract directly the geometric parameters of the pores in the original image, the results are not accurate. Therefore, the SEM or AFM image must be preprocessed. Usually the preprocessing includes two steps, digital binary image conversion and noise-reduce operation. With the first step, an original SEM or AFM image is converted to a digital binary image in which there are only two possible gray-scale values (0 or 1). In this paper, the conversion procedure is based on the thresholding method[22], an appropriate thresholding value is chosen according to the gray-scale histogram of the original image. Then two mathematical morphology operations, the erosion and dilation operations, are used to reduce noise in the binary image[22]. A typical SEM image of the nanoporous template and its noise-reduced digital binary image are shown in Fig. 1(a) and (b), respectively.

Porosity of template: For an M × N image, the corresponding binary image has the same size and its total pixel (N_t) is M × N. For the binary image, the white pixels stand for the pores in the nanoporous template and their gray-scale values are 0. After the number of white pixels (N_0) is counted, the porosity (P) of the template can be calculated as:

$$P = \frac{N_0}{N_t} \times 100\ \% \tag{1}$$

Diameters of pores: A set of the connected white pixels in the binary image is considered as a pore. To obtain the diameter of the ith pore (D_i), the boundaries of the ith pore in x and y axes, denoted as $x_{i,max}$, $x_{i,min}$, $y_{i,max}$ and $y_{i,min}$, must be identified firstly, then D_i is calculated as the following formulation:

$$D_i = \frac{(x_{i,max} - x_{i,min}) + (y_{i,max} - y_{i,min})}{2} \tag{2}$$

The average diameter ($\overline{D}$) of all pores can be expressed:

$$\overline{D} = \frac{\sum_{i=1}^{n} D_i}{n} \tag{3}$$

where n is the total number of pores, which is obtained by counting the sets of the connected white pixels.

Variance of diameters: The variance (S) of the diameters of all pores is an important parameter to characterize the uniformity of the pores in the nanoporous template, it can be easily calculated with eqn. 4:

$$S = \frac{\sum_{i=1}^{n} (D_i - \overline{D})^2}{n-1} \tag{4}$$

Quantification of ordering parameters: To analyze the orientational ordering of the pores in a nanoporous template, we convert its SEM or AFM image (morphology image) from the spatial domain to the frequency domain by 2-D fast Fourier transforms. 2-D fast Fourier transforms is a method to obtain the periodic information in the frequency domain which reflects the periodicity of an image in the spatial domain according to the gray-scale value of each pixel in the image[23,24]. Let f (x, y) express an M × N image (x = 0, 1, 2,. .., M-1 and y = 0, 1, 2,. .., N-1), the 2-D fast Fourier transforms of f, F (u, v), is given by the equation as follow[25]:

$$F(u,v) = \frac{1}{MN} \sum_{x=0}^{M-1} \sum_{y=0}^{N-1} f(x,y) \cdot \exp[-j2\pi(ux/M + vy/N)] \tag{5}$$

for u = 0, 1, 2, ..., M-1 and v =0, 1, 2, ..., N-1, where j is the imaginary unit.

The most important 2-D fast Fourier transforms result for an image is Fourier spectrum, which can be divided into four parts and has a centrosymmetric structure[26]. Usually, we will swap quadrants to move the origin of the transform to the center of the frequency rectangle and obtain a centered Fourier spectrum[22]. The typical centered Fourier spectrum for a nanoporous template (Fig. 1a) is shown in Fig. 1c, in which there are some bright spots at special positions and the similar pattern of the bright spots contains the spatial periodicity

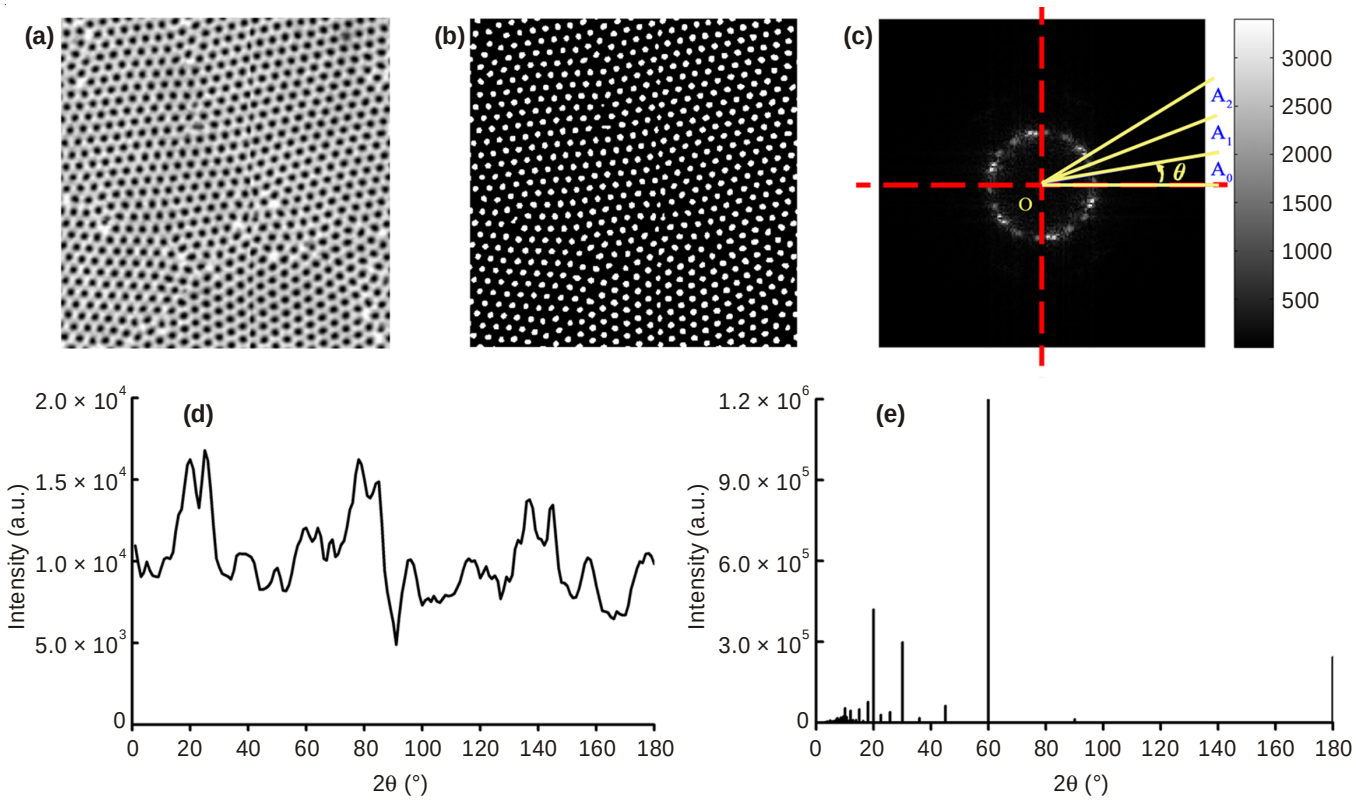

Fig. 1. (a) A typical morphology of an anodic aluminum oxide template; (b) The binary image of the anodic aluminum oxide template after image preprocessing; (c) The centered Fourier spectrum for the anodic aluminum oxide template. The radials OA_0, OA_1, OA_2, …, OA_{Nd} are drawn with the angle interval of θ. (d) The angle distribution curve of the bright spots in the centered Fourier spectrum; (e) 1-D fast Fourier transforms results of the angle distribution curve

information of the template. According to the patterns, Rahimi *et al*.[21] and Zhang *et al*.[27] obtained useful qualitative information about the ordering of pores in nanoporous template, respectively.

Here, we propose a method to extract quantitatively the orientational ordering parameters of the pores in nanoporous templates according to the pattern of the bright spots in the centered Fourier spectrum. In order to obtain the exact positions of the bright sports, firstly we let the center of the centered Fourier spectrum as the polar and set up a polar coordinate system, then we draw N_d radials OA_0, OA_1, OA_2, …, OA_{Nd} with an angle interval of θ (θ = 180°/N_d). After the sums of the brightness of every pixel along each radial OA_1, OA_2, …, OA_{Nd} are calculated respectively, the angle distribution curve of the bright spots is obtained as shown in Fig. 1d. It is noteworthy that the above calculation within the angle range from 0 to 180° due to the centrosymmetry of the Fourier spectrum.

The angle distribution curve of bright spots (Fig. 1d) is not intuitively clear and it is difficult to find its exact period. Considering 1-D fast Fourier transforms is a powerful technique to extract the period information of periodical signals[22], we employ further 1-D fast Fourier transforms to analyze the angle distribution curve of the bright spots and the results are shown in Fig. 1e. In Fig. 1e, there is a highest peak locates at a special angle (we call this angle characteristic angle) and according to this angle the lattice type of the template could be inferred. For example, in Fig. 1e, the characteristic angle is 60.0°, which means that the period of the angle distribution is 60.0°. Since 360°/60° = 6, it could be concluded that the arrangement of the bright spots in the centered Fourier spectrum in Fig. 1c exhibits a 6-fold axis of rotation symmetry and the arrangement of pores in the nanoporous templates as shown in Fig. 1a belongs to a hexagonal lattice.

If we analyze the 1-D fast Fourier transforms further, we will obtain more information about the orientational ordering of the pores and this information can be used to evaluate the quality of the template. In the 1-D fast Fourier transforms result, besides the highest peak locates at the characteristic angle, there are several lower peaks. According to the principle of 1-D fast Fourier transforms, the second highest peak should locate at the half of the characteristic angle exactly with the 0.25 (1/4) amplitude of the highest peak. If the positions and amplitudes of the peaks are in accordance with this rule, it means that the quality of the corresponding nanoporous template is very good. Therefore, we can assess the quality of a template by checking the position and the amplitude of the second highest peak in the 1-D fast Fourier transforms. Here we name a parameter peak-peak ratio (PPR) as the ratio of the amplitude of the second highest peak to that of the highest peak:

$$\text{Parameter peak-peak ratio (PPR)} = \frac{P_{shp}}{P_{hp}} \quad (6)$$

where P_{shp} and P_{hp} are the amplitudes of the second highest peak and the highest peak, respectively.

The procedures and programming algorithm mentioned above are illustrated as a flow chart in Fig. 2.

The algorithm is accomplished using MATLAB, which is a widely used programming software in the physical and

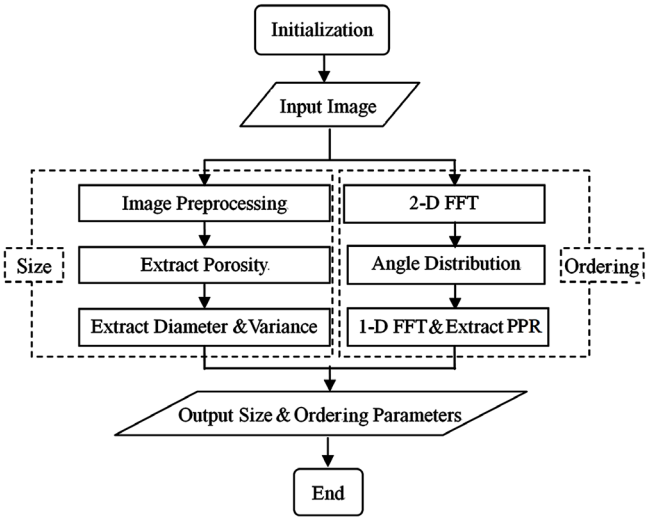

Fig. 2. Flow chart of the program

engineering sciences. In the program, a lot of built-in functions can be fully utilized such as *bw morph* for noise-reduce operation, *bw label* for connected components detection, *fft2* for 2-D fast Fourier transforms computation and *fft* for 1-D fast Fourier transforms computation. According to the trustworthy calculation of numerical value and powerful functions of MATLAB, the algorithm can be realized more reliable and efficient. It can also be modified by users and integrated easily to the C language and many other programming languages.

Algorithm validation: To verify the reliability and accuracy of our method and program, a standard test image shown in Fig. 3a is analyzed. The standard test image is constructed by MATLAB with such features: (i) The image includes 512 × 512 pixels, which is the typical size of an SEM image. (ii) There are 22 pores arranged in the hexagonal lattice with preset centers and diameters, which are listed in the first lines of Table-1. (iii) Each pore is filled in gray with different level, considering that the SEM image is the gray-scale image. It is noteworthy that the unit of the program is based on pixel, which can be transferred to any practical unit according to the scale of the original image if necessary.

As illustrated in the last line of Table-1, all geometric parameters of the stand test image extracted with our program agree very well with the preset values although the porosity has small relative error because of sawtooth border around the edge of pores.

Fig. 3b shows the centered Fourier spectrum corresponding to the image of Fig. 3a. In Fig. 3b, it is clear that six distinct spots locate along the edges of a hexagon, which indicates that the pores in Fig. 3a have an orderly arrangement.

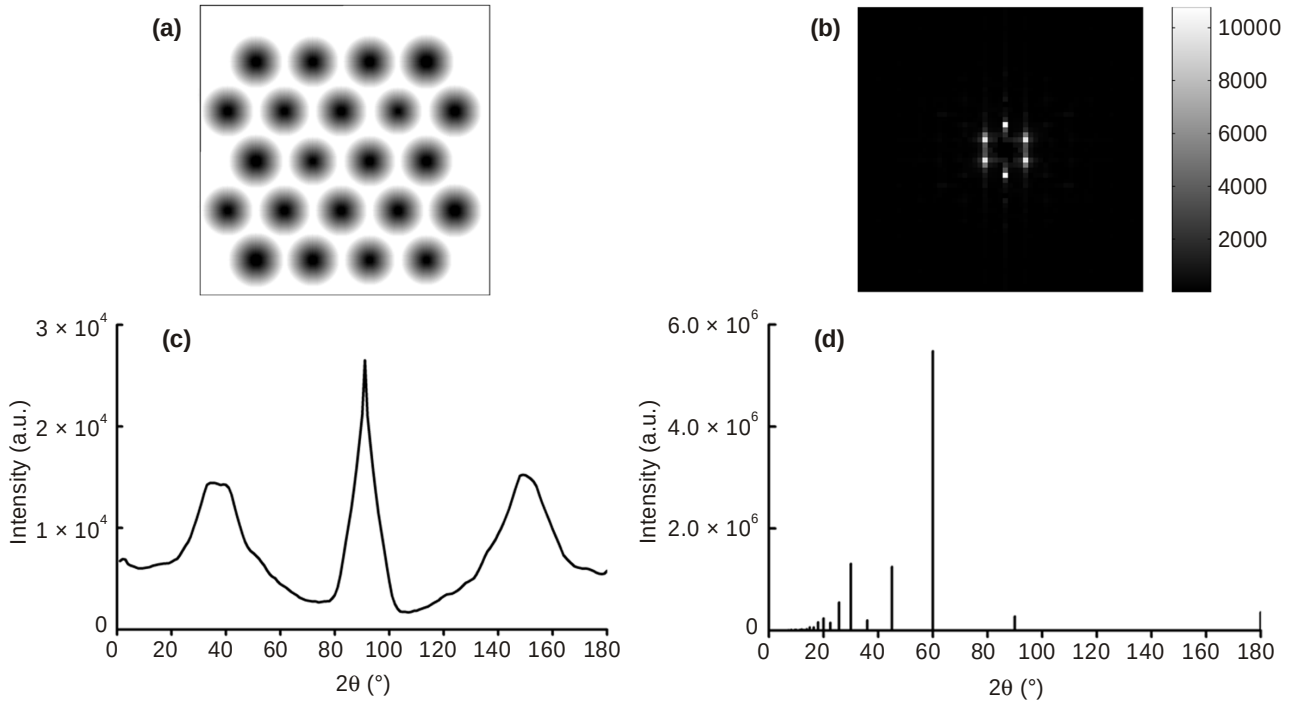

Fig. 3. (a) The standard test image with 22 pores; (b) 2-D fast Fourier transforms pattern; (c) The angle distribution curve of (b), calculated with the intensity magnitude form 0 to 180° at step size of 1°; (d) 1-D fast Fourier transforms results of (c)

TABLE-1
PRESET PARAMETERS AND ANALYSIS RESULTS FOR THE STANDARD TEST IMAGE

Preset parameters	Pores (diameter × number)							Diameter		Porosity (%)	Characteristic angle (°)	Peak-peak ratio
								Average (pix.)	Variance			
Preset values	84×1	86×1	88×4	90×7	92×5	94×2	96×2	90.55	8.83	54.09	60	0.25
Analysis results	84×1	86×1	88×4	90×7	92×5	94×2	96×2	90.55	8.83	55.47	60	0.24
Relative error	0	0	0	0	0	0	0	0	0	2.55	0	0.04

The angle distribution curve of the bright spots in Fig. 3b is calculated as the description as above at the step size of 1° and the results are shown in Fig. 3c. Then 1-D fast Fourier transforms is employed to analyze the angle distribution curve and the results are shown in Fig. 3d. In Fig. 3d, we can find that the characteristic angle corresponding to the highest peak is 60° and the second highest peak locates at 30° with the peak-peak ratio value of 0.24, indicating that the pores arrange orderly and the lattice type of the pores in the standard test image is hexagonal, which is agreed with the preset values.

According to the results, the geometric parameters of the standard test image, including the porosity, the diameter and their variance, are calculated by our algorithm accurately and efficiently. Moreover, the characteristic angle and peak-peak ratio of the pores arrangement in the standard test image is extracted quantitatively and then the lattice type is inferred reliably.

RESULTS AND DISCUSSION

We will analyze several SEM images of anodic aluminum oxide nanoporous templates with our method.

As the first example, we will compare the quality of a small-area ordered anodic aluminum oxide template (Fig. 4a) with that of a large-area one (Fig. 4d)[28]. For the former, its centered Fourier spectrum consists of distinct spots (Fig. 4b), the second highest peak locates at 30° and peak-peak ratio is 0.21 (Fig. 4c), which indicates the fairly good periodicity. But for the large-area template, there are usually large numbers of pores with different orientations and the corresponding centered Fourier spectrum will change to a ring[21] (Fig. 4e). The corresponding angle distribution curve of Fig. 4e, the ring-shape centered Fourier spectrum, is much complex and there are two peaks with close amplitudes in the 1-D fast Fourier transforms results (Fig. 4f). In Fig. 4f, although the second highest peak locates at 30°, peak-peak ratio is about 0.97, which is much larger than the theoretical value 0.25. Therefore, we can draw a conclusion that the former template, the small-area one, is better. The analysis results are shown in Table-2.

In the above example, the differences of the two nano-templates in the long-range are very obvious. Here we analyzed another example, two anodic aluminum oxide templates. They were fabricated by anodization process under the similar preparation conditions, so that their morphology images were too similar to distinguish which one is better with unaided eyes. The images of the two anodic aluminum oxide templates are selected from the reference[29] and shown in Fig. 5a and Fig. 5c, respectively. Although the resolution of the images is not very high, the size and angle parameters shown in Table-3 can be extracted using our program successfully and used to assess the quality of the two templates.

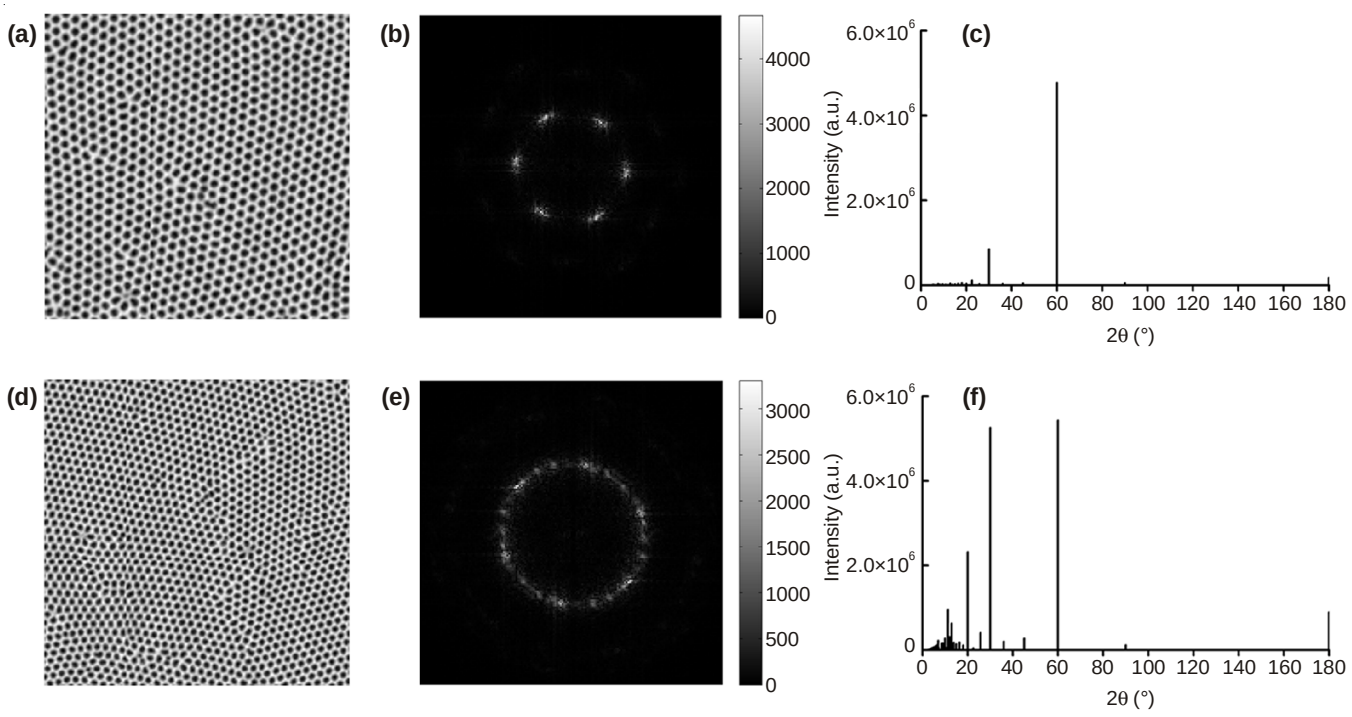

Fig. 4. (a),(d) The SEM image of anodic aluminum oxide template. Reproduced with permission [Ref. 28], (b),(e) 2-D fast Fourier transforms pattern of (a),(d), respectively; (c), (f) 1-D fast Fourier transforms results of (b),(e), respectively

TABLE-2
ANALYSIS RESULTS OF SEM IMAGES OF ANODIC ALUMINUM OXIDE TEMPLATES

Image	Porosity (%)	Diameter		Characteristic angle (°)	Location of the second highest peak (°)	Peak-peak ratio
		Average (pix.)	Variance			
Fig. 4a	38.45	7.41	0.31	60.0	90.0	0.21
Fig. 4d	38.71	5.54	0.35	60.0	90.0	0.97

According to the analysis results, the porosity and average diameter of the pores in Fig. 5a are very close to those in Fig. 5c. However, the diameter variance of the pores in Fig. 5c is smaller than that in Fig. 5a, suggesting that the pores in Fig. 5c are more homogeneous in size. Additionally, based on the 1-D fast Fourier transforms patterns shown in Fig. 5b and Fig. 5d, both the characteristic angles of the two templates are quite the same value (60°), which indicates that the arrangement of the pores in the two templates is hexagonal lattice. The second highest peak in Fig. 5b locates at 90° instead of 30° while the second highest peak in Fig. 5d locates at 30° (the exact half of the characteristic angle), which indicates that the arrangement of the pores in the template of Fig. 5c is more regularly than that of Fig. 5a. Thus, due to homogeneous size and orderly arrangement, we can draw a conclusion that the quality of template in Fig. 5c is better, so the preparation condition of template in Fig. 5c is more favourable for high-performance functional materials.

Our method is not only suitable for hexagonal lattice and circular pores, but also effective for other lattices or non-circular pores. As the third example, we analyzed a template of the non-circular pores with different lattices, which is illustrated in Fig. 6a. This anodic aluminum oxide template was fabricated by the artificial laying-out of the initiation sites of holes in square graphite structure lattices[30]. Employing our method, the angle parameters are extracted successfully. The results are shown in Fig. 6b, the characteristic angles of the template is 90°, demonstrating clearly the type of lattice is square.

Conclusion

In this paper, a facile and accurate method to evaluate the quality of nanoporous templates is presented. By using the image processing technology, the geometric parameters of nanoporous templates including the porosity, diameters and their variance of pores are extracted and these parameters can be used to assess the homogeneity of the pores in the templates. To evaluate the ordering of the pores in the nanoporous temples, an approach combines 2-D fast Fourier transforms and 1-D fast Fourier transforms techniques is proposed and

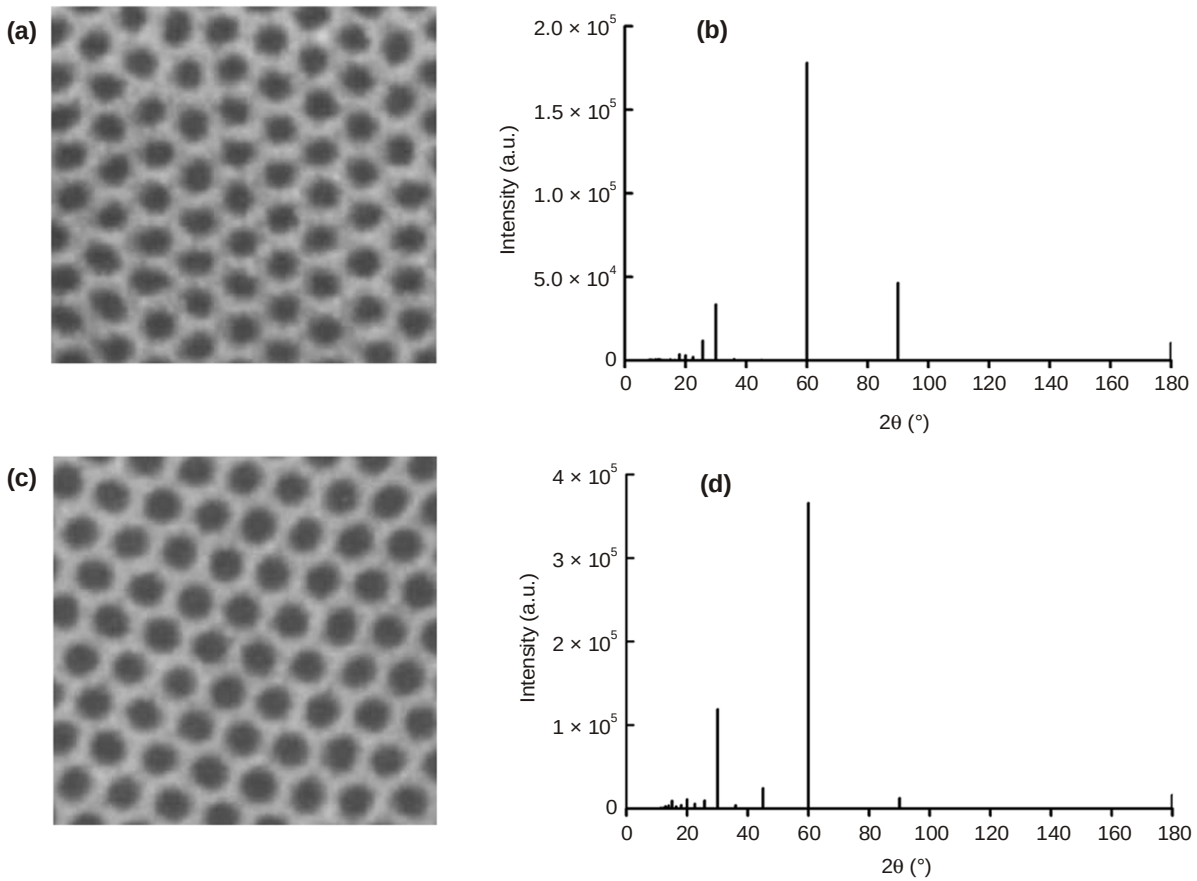

Fig. 5. (a) SEM image of an anodic aluminum oxide template (U = 25V, 0.3M H_2SO_4, t = 706 min); (b) 1-D fast Fourier transforms results of (a); (c) SEM image of an anodic aluminum oxide template (U = 27V, 0.3M H_2SO_4, t = 450 min). Reproduced with permission [Ref. 29]; (d) 1-D fast Fourier transforms results of (c)

TABLE-3
ANALYSIS RESULTS OF SEM IMAGES OF ANODIC ALUMINUM OXIDE TEMPLATES

Image	Porosity (%)	Diameter		Characteristic angle (°)	Location of the second highest peak (°)	Peak-peak ratio
		Average (pix.)	Variance			
Fig. 5a	43.43	21.09	2.05	60.0	90.0	0.26
Fig. 5c	43.70	21.77	1.58	60.0	30.0	0.32

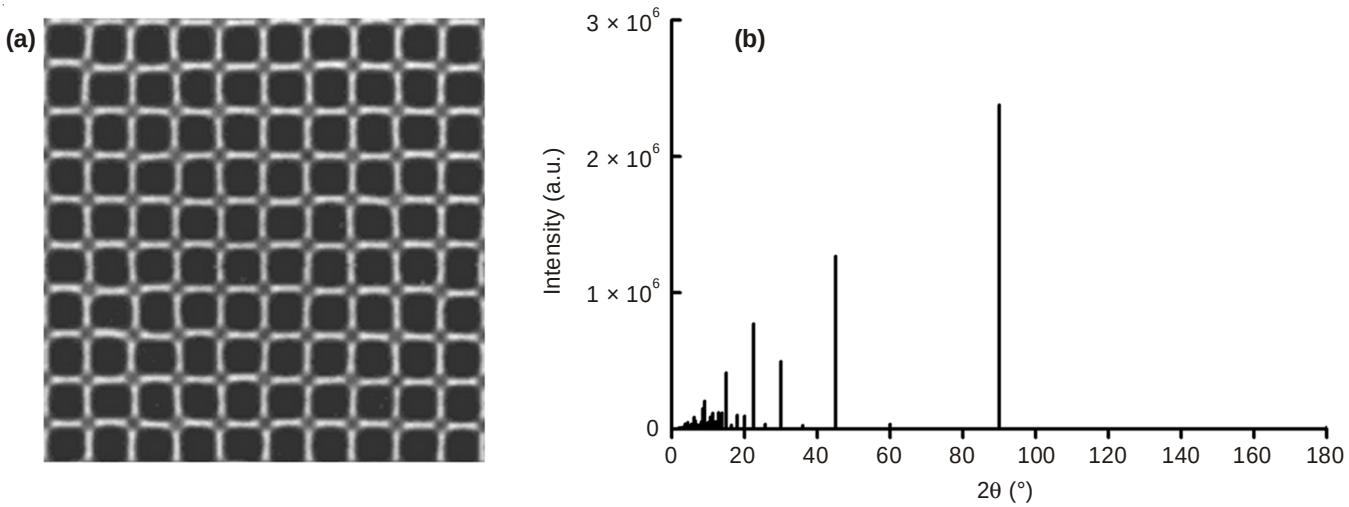

Fig. 6. (a) SEM image of a square anodic aluminum oxide template. Reproduced with permission [Ref. 30]; (b) 1-D fast Fourier transforms results

the parameters of the characteristic angle and peak-peak ratio are calculated. According to the characteristic angle and peak-peak ratio, the lattice type and orientations of pores arrangement can be inferred. This method was programmed in MATLAB environment and its accuracy and reliability were verified by analyzing a standard test image. As the applications, the program was used to evaluate the quality of nanoporous templates comprehensively and quantitatively, not only for the pore ordering is in the short-range but also for the long-range and no matter whether the lattice is hexagonal lattice or not. The rapid and reliable evaluation of the quality of the nanoporous templates will be beneficial to optimize the templates preparation conditions for the high-performance functional nanomaterials in the future.

ACKNOWLEDGEMENTS

The authors acknowledge the financial support from the National Natural Science Foundation of China (21373281, 21273293), the Program of China Scholarships Council (No. 201406055006), the Program for New Century Excellent Talents in University (NCET-13-0633, NCET-12-0587), the Project for Distinguished Young Scholars in Chongqing (cstc2014jcyjjq100004), the Fundamental Research Funds for the Central Universities (CDJXS12222254, CDJZR13225501) and the sharing fund of Chongqing University's Large-scale Equipment.

REFERENCES

1. F.I. Dar, S. Habouti, R. Minch, M. Dietze and M. Es-Souni, *J. Mater. Chem.*, **22**, 8671 (2012).
2. J.J. Li and L.T. Zhang, *Asian J. Chem.*, **24**, 4130 (2012).
3. Z.Y. Zeng, X. Huang, Z.Y. Yin, H. Li, Y. Chen, H. Li, Q. Zhang, J. Ma, F. Boey and H. Zhang, *Adv. Mater.*, **24**, 4138 (2012).
4. B. Sun, Y.Z. Hao, F. Guo, Y.H. Cao, Y.H. Zhang, Y.P. Li and D.S. Xu, *J. Phys. Chem. C*, **116**, 1395 (2012).
5. D. Xu, X.H. Yan, P. Diao and P.G. Yin, *J. Phys. Chem. C*, **118**, 9758 (2014).
6. A. Huczko, *Appl. Phys., A Mater. Sci. Process.*, **70**, 365 (2000).
7. W. Lee and S. Park, *Chem. Rev.*, **114**, 7487 (2014).
8. J.J. Li, J.B. Zhang, L.T. Zhang, Y. Liu and W.C. Hao, *Asian J. Chem.*, **25**, 6173 (2013).
9. X.W. Kang and S.W. Chen, *J. Mater. Sci.*, **45**, 2696 (2010).
10. Y.C. Liu and K.Y. Xie, *Sci. Adv. Mater.*, **6**, 863 (2014).
11. J.K. Chang, S.H. Hsu, W.T. Tsai and I.W. Sun, *J. Power Sources*, **177**, 676 (2008).
12. D.Y. Ding, Z. Chen, S. Rajaputra and V. Singh, *Sens. Actuators B*, **124**, 12 (2007).
13. G.E. Thompson, *Thin Solid Films*, **297**, 192 (1997).
14. N. Hassanzadeh, H. Omidvar, M. Poorbafrani and S.H. Tabaian, *Arab J. Sci. Eng.*, **38**, 1305 (2013).
15. R. Hillebrand, F. Muller, K. Schwirn, W. Lee and M. Steinhart, *ACS Nano*, **2**, 913 (2008).
16. A.C. Johnston-Peck, J. Wang and J.B. Tracy, *Langmuir*, **27**, 5040 (2011).
17. M.J. Abdollahifard, K. Faez, M. Pourfard and M. Abdollahi, *Appl. Surf. Sci.*, **257**, 10443 (2011).
18. M. Pourfard, K. Faez and S.H. Tabaian, *J. Phys. Chem. C*, **117**, 17225 (2013).
19. J.R. Borba, C. Brito, P. Migowski, T.B. Vale, D.A. Stariolo, S.R. Teixeira and A.F. Feil, *J. Phys. Chem. C*, **117**, 246 (2013).
20. L. Zaraska, G.D. Sulka, J. Szeremeta and M. Jaskula, *Electrochim. Acta*, **55**, 4377 (2010).
21. M.H. Rahimi, S.H. Tabaian, S.P.H. Marashi, S. Saramad, M. Arab and A. Hemasian, *Micro & Nano Lett.*, **7**, 125 (2012).
22. R.C. Gonzalez, R.E. Woods and S.L. Eddins, Digital Image Processing Using Matlab, edn 4, Prentice Hall Publisher, New York (2004).
23. E. Aubert and C. Lecomte, *J. Appl. Cryst.*, **40**, 1153 (2007).
24. X.Y. Su and W.J. Chen, *Opt. Lasers Eng.*, **35**, 263 (2001).
25. R.C. Gonzalez and R.E. Woods, Digital Image Processing, edn 2, Prentice Hall, New York (2002).
26. I. Amidror, Mastering the Discrete Fourier Transform in One, Two or Several Dimensions, edn 1, Springer London Ltd, England (2013).
27. G.L. Zhang, L.X. Jin, P. Zheng, W. Wang and X.-J. Wen, *Chinese J. Polym. Sci.*, **31**, 798 (2013).
28. K.S. Napolskii, I.V. Roslyakov, A.A. Eliseev, A.V. Petukhov, D.V. Byelov, N.A. Grigoryeva, W.G. Bouwman, A.V. Lukashin, K.O. Kvashnina, A.P. Chumakov and S.V. Grigoriev, *J. Appl. Cryst.*, **43**, 531 (2010).
29. H. Masuda, F. Hasegawa and S. Ono, *J. Electrochem. Soc.*, **144**, L127 (1997).
30. H. Masuda, H. Asoh, M. Watanabe, K. Nishio, M. Nakao and T. Tamamura, *Adv. Mater.*, **13**, 189 (2001).